THE ASTROPHYSICAL JOURNAL, 433:L37–L40, 1994 September 20

REGIMES OF HIGH-ENERGY SHOCK EMISSION FROM THE Be STAR/PULSAR SYSTEM PSR 1259−63

MARCO TAVANI,[1] JONATHAN ARONS,[2] AND VICTORIA M. KASPI[1]
Received 1993 December 31; accepted 1994 June 6

ABSTRACT

PSR B1259−63 is a 47 ms radio pulsar in a wide, eccentric orbit with a Be star. We study the shock interaction between the pulsar and the companion's mass outflow and investigate the time evolution of radiative shock regimes. We find that for small values of the Be star's mass-loss rate, inverse-Compton scattering is likely to dominate the shock emission. Alternately, for a large mass-loss rate, synchrotron emission will dominate. Multifrequency X-ray and gamma-ray observations near periastron can distinguish between these cases and yield unique constraints on the pulsar and Be star winds. The PSR B1259−63 system provides a unique laboratory to study the time-dependent interaction of a pulsar wind with the circumbinary material from its companion star.

Subject headings: gamma rays: theory — pulsars: individual (PSR B1259−63) — stars: emission-line, Be — X-rays: stars

1. INTRODUCTION

PSR B1259−63 is the first radio pulsar found orbiting a massive nondegenerate stellar companion (Johnson et al. 1992). The pulsar has spin period $P = 47.76$ ms, period derivative $\dot{P} = 2.279 \times 10^{-15}$, and spin-down luminosity $\dot{E}_R \simeq 9 \times 10^{35}$ ergs s^{-1}. The orbital period is $P_{\rm orb} = 3.4$ yr and orbital eccentricity $e = 0.87$ (Johnston et al. 1994). Its companion is SS 2883, a 10th mag Be star of luminosity $L_0 = 5.8 \times 10^4$ $L_\odot$, with estimated radius $R_* \sim 11\ R_\odot \sim 8 \times 10^{11}$ cm and an estimated distance from Earth of 3 kpc. Be stars are characterized by high-density mass outflows in the stellar equatorial plane, and the wide orbit and high eccentricity of the PSR B1259−63 system provide highly variable physical regimes for interaction between the pulsar and Be star winds (e.g., Kochanek 1993, King 1993). The system was detected near apastron in the soft X-ray band by *ROSAT* when the radio pulsations were still visible (Cominsky, Roberts, & Johnston 1994). Interaction between the pulsar wind and circumbinary material can produce X-ray emission. Here we show that the time variation of the pulsar cavity and shock results in observably different radiative regimes as a function of orbital phase and stellar wind parameters. X-ray and gamma-ray observations near periastron (1994, January 9) can test the model presented here. A more comprehensive study will appear elsewhere.

2. FORMATION OF A PULSAR WIND TERMINATION SHOCK

The high-density equatorial disk wind region in Be stars has a density profile $\rho(R)$ derived from the IR excess of the form $\rho(R) = \rho_0 (R/R_*)^{-n'}$, where R_* is the radius of the star (Waters et al. 1988), R is the distance from its surface, and $\rho_0 = \dot{M}/(4\pi f R_*^2 v_0)$, with $\dot{M}$ being the mass outflow rate, v_0 the outflow velocity at the surface of the Be star, and f the fraction of 4π sr into which the mass loss occurs. Observations of Be stars indicate that $f \lesssim 1$ with the mass outflow concentrated in the equatorial plane (Waters 1986). For simplicity, we assume that the Be star equatorial plane coincides with the pulsar orbital plane. Typically, the surface density ρ_0 is of the order of 10^{-12}–10^{-11} g cm^{-3}, and the "outflow exponent" is in the range $2 < n' < 4$ (Waters et al. 1988). The pressure has a radial dependence of the form $P(R) = \rho(R) v(R)^2 \propto (R/R_*)^{n'-4}$, obtained with the use of the continuity equation in spherical symmetry. Note that the outflow velocity changes with distance as $(R/R_*)^{n'-2}$, i.e., it increases for $n' > 2$ as suggested by Be outflow observations (Waters et al. 1988). It is useful to define the mass outflow parameter,[3] $\Upsilon = \dot{M}_{-8} v_{0,6}$, where $\dot{M} = (10^{-8}\ M_\odot\ {\rm yr}^{-1})\dot{M}_{-8}$, and $v_0 = (10^6\ {\rm cm\ s}^{-1}) v_{0,6}$. We parameterize the properties of the Be star mass outflow by specifying the couple of parameters (Υ, n').

A shock region will form as a result of the interaction of the pulsar wind from PSR B1259−63 with the mass outflow from its Be star companion. A relativistic pulsar wind has a flow rate in ions $\dot{N}_i$ and in $e^\pm$ pairs $\dot{N}_\pm$, a flow Lorentz factor γ_1, and a ratio of the magnetic energy flux to kinetic energy flux upstream of the shock, σ. The MHD model of the pulsar wind in the Crab Nebula implies $\sigma \sim 0.005$ (Kennel & Coroniti 1984). In the Crab pulsar, fully stripped ions of relatively low charge ($Z \sim 2$) probably carry most of the wind's inertia and have been accelerated to a fraction $\eta \sim 0.3$ of the open field line voltage of the neutron star (Gallant & Arons 1994). For PSR B1259−63 the voltage across the open field lines is $\Phi_c \sim (4\dot{E}_R/c)^{1/2} \simeq 10^{15}$ V. We assume that the ions in the wind from PSR B1259−63 have experienced the same fraction of the voltage drop across the open magnetosphere as in the Crab Nebula. Then the upstream Lorentz factor at the shock is $\gamma_1 = \eta Z e \Phi_c/(m_i c^2) \simeq 4 \times 10^6 \eta$, with m_i being the average ion mass.

The radial distance r_s from the pulsar of the apex of the shock region is obtained by equating the pulsar radiation pressure with the ram pressure of the Be star outflow (e.g., Arons &

[1] Joseph Henry Laboratories and Physics Department, Princeton University, Princeton NJ 08544.
[2] Astronomy Department and Physics Department, University of California at Berkeley, Berkeley, CA 94720.

[3] We use the notation X_p, for a physical quantity in units of 10^p.

Tavani 1993). The radius r_s is the solution of the equation,

$$\frac{r_s/d(\theta)}{\{1-[r_s/d(\theta)]\}^{2-n'/2}} = \left(\frac{\dot{E}_R f}{c\dot{M}v_0}\right)^{1/2}\left[\frac{R_*}{d(\theta)}\right]^{n'/2-1} \simeq \frac{7.2f^{1/2}}{\Upsilon^{1/2}}\left[\frac{R_*}{d(\theta)}\right]^{n'/2-1}, \quad (1)$$

where we have assumed $R_* \ll d$, with d being the pulsar–Be star separation. In general, r_s is a function of the true anomaly θ, n', and Υ. Figure 1*a* shows r_s as a function of orbital phase obtained from equation (1) for different Υ values and for $n' = 3$. Periastron is at $\theta = 180°$. The relatively large value of the shock radius along the line of centers between the stars (always close to d) suggests that PSR B1259−63 will not develop a wind-fed accretion powered pulsar even at periastron, unless $\Upsilon \gg 1$ and $3 \lesssim n' \lesssim 4$. This conclusion follows from the fact that the gravitational accretion radius $R_G \equiv 2GM_p/v_*^2 \approx (3 \times 10^{12}\ \mathrm{cm})M_{p,1.4}/v_{*,7}^2$ [with $M_{p,1.4}$ being the pulsar mass in units of 1.4 $M_\odot$ and $v_{*,7} = v_*/(10^7\ \mathrm{cm\ s^{-1}})$, where $v_* = \sqrt{v^2 + v_{\mathrm{orb}}^2}$, and v_{orb} is the orbital velocity] is small compared to r_s for a broad range of Υ and n'. Roche mass transfer never occurs, since for a 10 $M_\odot$ Be star, the star's surface gravity exceeds the pull from the pulsar by a factor of $\sim 4 \times 10^4$ even at closest approach, where $d_{\min} \approx 23\ R_\odot$. However, the effects of radio pulse dispersion and absorption as the pulsar passes into the densest part of the outflow may cause the radio signal to drop out at periastron.

The magnetic field in the pulsar wind at the shock distance corresponding to the apex of the pulsar cavity is $B_1(r_s) = [\sigma/(1+\sigma)]^{1/2}(\dot{E}_R/r_s^2 c f_p)^{1/2}$, with f_p being the fraction of the total solid angle for the pulsar wind expansion ($f_p = 1$ for isotropic expansion). Note that $B_1(r_s)$ depends ultimately on the value of the gas pressure at r_s and, to first order, is independent of the pulsar spin-down power. Figure 1*b* gives the behavior of $B_1(r_s)$ as a function of θ for different values of Υ.

The wind stops in a relativistic shock wave, located just interior to the pulsar wind cavity. Behind the shock, the magnetic field settles down to $B_2 = 3B_1$. We assume the geometry of a perpendicular shock, with an upstream magnetic field perpendicular to the shock normal. Our treatment of shock acceleration and high-energy emission has general validity with the assumption of a power-law distribution of postshock $e^\pm$ pairs. However, we make use of the detailed calculations of Hoshino et al. (1992), who derive the $e^\pm$ pair distribution from shock acceleration theory.

3. SHOCK RADIATIVE REGIMES

The luminosity and spectrum of high-energy shock radiation depend on the various radiative timescales and their relation to the flow timescale. The flow time of particles streaming with velocity $V_f \sim c/3$ behind the nebular shock is $\tau_f \simeq r_s/V_f \simeq 50\ [1/(n_{10} f_p v_7^2)]^{1/2}[(c/3)/V_f]$ s. Figure 1*c* gives the numerical values of τ_f as a function of θ and Υ. The acceleration time τ_a for nonthermal magnetosonic acceleration of $e^\pm$ pairs at and near the transverse shock front is $\tau_a \sim \Omega_i^{-1} = m_i c\gamma_1/(ZeB_2) \sim 10^2(\gamma_{1,6}/ZB_2)$ s, where Ω_i is the ion's relativistic cyclotron frequency at the shock front (Arons 1994). Detailed numerical calculations by Hoshino et al. (1992) have shown that the $e^\pm$ pairs, in the absence of radiative losses, acquire a nonthermal energy distribution $N(\gamma) \propto \gamma^{-s}$ for $\gamma_1 < \gamma < \gamma_m$. The simulations show that $s \sim 2$, and a fraction $\epsilon_a \sim 0.2$ of the flow energy flux goes into the final energy of the nonthermal pairs, when radiative losses are unimportant. We note that in the case of PSR B1259−63, because of the rapid cooling of the shocked relativistic particles, near periastron the downstream γ-factor never reaches the value $\gamma_m = \gamma_1 m_i/(Zm_\pm)$ obtainable without appreciable radiative cooling. Only far from periastron it is possible for the downstream γ-factor to be near γ_m.

Radiative losses of the $e^\pm$ pairs due to synchrotron radiation in the local magnetic field and inverse-Compton scattering (IC)

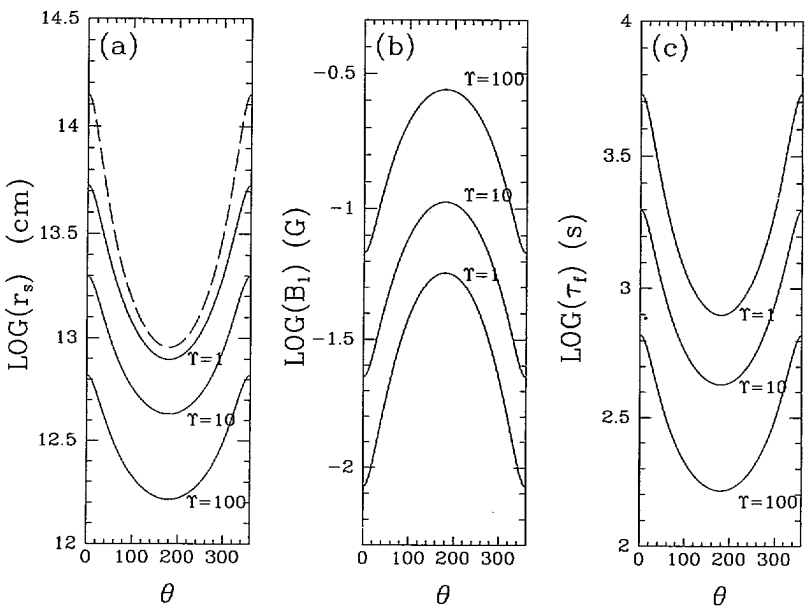

FIG. 1.—Logarithm of (*a*) shock radius r_s from pulsar and orbital separation (*dashed curve*) from eq. (1), (*b*) magnetic field at the shock B_1, and (*c*) flow time τ_f of particles behind the shock as a function of the true anomaly θ for different values of the mass-loss parameter $\Upsilon = \dot{M}_{-8} v_{0.6}$. Periastron is at $\eta = 180°$. We assume $n' = 3$ and an inclination angle of 36° corresponding to a Be star mass of 10 $M_\odot$.

in the background IR, optical, and UV radiation field originating from the Be star surface limit the maximum Lorentz factor attainable at the shock. The synchrotron loss time is $\tau_s(\gamma) = 3m_\pm^3 c^5/(e^4 B_2^2 \gamma) \sim 1.3 \times 10^3 (\gamma_6 B_2^2)^{-1}$ s. The IC cooling timescale of high-energy $e^\pm$ pairs against photons in the Thomson regime ($\gamma\epsilon \ll m_\pm c^2$, with ϵ being the photon energy) is $\tau_c = (U_B/U_p)\tau_s$, where U_B is the energy density of the postshock electromagnetic field, and U_p is the energy density of the Be star radiation. The electromagnetic energy density at r_s is then $U_B(r_s) = B_2^2(r_s)/8\pi$, and the photon energy density is $U_p = R_*^2 \sigma_B T^4 (\bar{R}_s^2 c)$, where σ_B is the Stefan-Boltzmann constant, T is the Be star's effective temperature, and $\bar{R}_s$ is the distance between the closest point on the surface of the Be star and the shock. The above formulae are valid only in the Thomson regime and in the case of a radiation bath at the photospheric temperature of the Be star ($T \simeq 27{,}000$ K $\simeq 2.3$ eV). This approximation is valid *only for* $\gamma_1 \lesssim 10^5$. However, for a typical Crab-like Lorentz factor ($\gamma_1 \sim 10^6$), Compton scattering occurs in the relativistic regime, and it is necessary to take into account the Klein-Nishina decrease of the cross section as a function of center-of-mass energy. The dimensionless parameter characterizing the scattering is (Blumenthal & Gould 1970) $\Gamma_\epsilon = 4\gamma\bar{\epsilon}/(m_\pm c^2)$, with $\bar{\epsilon} = 2.7 k_B T$ being the average photon energy of the radiation blackbody field, and k_B being Boltzmann's constant. In the case of PSR B1259−63, $\Gamma_\epsilon \sim 50\gamma_{1,6}$. The Thomson approximation can be used for $\Gamma_\epsilon \lesssim 1$, but it is clearly not applicable if $\gamma_{1,6} \sim 1$. It can be shown that the ratio of the IC scattering timescale in the Klein-Nishina regime $\tau_{c,r}$ to the Thomson timescale τ_c with $\gamma_1 \sim 10^6$ is $\tau_{c,r}/\tau_c \gtrsim 10$.

Different radiative regimes exist at the shock for different combinations of timescales. A value of τ_a small compared with other relevant timescales is required to accelerate the $e^\pm$ pairs and produce a nonthermal power-law distribution of $e^\pm$ at the shock with energies $\gamma > \gamma_1$. On the other hand, cooling by synchrotron and IC emission limits the nonthermal shock acceleration. The total cooling rate per radiating $e^\pm$ pair at the shock τ_r^{-1} can be written as $\tau_r^{-1} = \tau_s^{-1} + \tau_c^{-1}$. If τ_r is long compared with τ_f, the radiative losses are negligible, the flow is adiabatic, and the resulting radiation nebula is *diffuse* (e.g., Arons & Tavani 1993). If the cooling timescale τ_r is short compared to τ_f, the shock acceleration of pairs produces a spectrum of $e^\pm$ which is cut off at high energy, and a *compact* nebula forms. Finally, if $\tau_a \gg \tau_r$, no nonthermal acceleration is possible at the shock, and the emerging spectrum is dominated by the cooling mechanism with the largest rate.

The maximum Lorentz factor γ_m^* that can be achieved by nonthermal acceleration of ions' magnetosonic waves at the shock is obtained from the condition $\tau_s(r_s)/\tau_a(r_s) \sim (\gamma_m^* \gamma_1)^{-1}$, which is substantially smaller than γ_m obtained in the absence of radiative losses. Thus, we can study the different radiation regimes by considering the set of ratios of timescales τ_s/τ_c, τ_a/τ_s, τ_a/τ_c that are characteristics of the shock emission. We plot in Figure 2 these ratios for different values of θ and Υ. For PSR B1259−63, τ_c can be much smaller than τ_s near periastron for a large variety of outflow parameters. IC scattering therefore dominates the cooling processes at periastron unless the shock is relatively close to the pulsar. This happens for $\Upsilon \gtrsim 10^3$ (Fig. 2). A pulsar-driven shock radiative regime dominated by IC cooling due to optical star emission scattering has not been studied previously.

4. INTENSITY AND SPECTRAL PROPERTIES OF THE SHOCK EMISSION

4.1. *Nonthermal "Diffuse" Nebular Emission*

This is the case characterized by $\tau_a \ll \tau_f \ll \tau_s, \tau_c$. This case applies to the part of the pulsar orbit far from the Be star for a broad range of input outflow parameters. Except for cases with $1 \lesssim \Upsilon \lesssim 10$ (with $n' = 3$, and $\sigma \gg 1$), synchrotron cooling dominates the emission near apastron, i.e., near $\theta = 0$ (see Fig. 2). Since the flow time in the shock front is much less than the synchrotron loss time in the downstream flow, the flow is adiabatic both in the ions and in the pairs. Therefore, the resulting

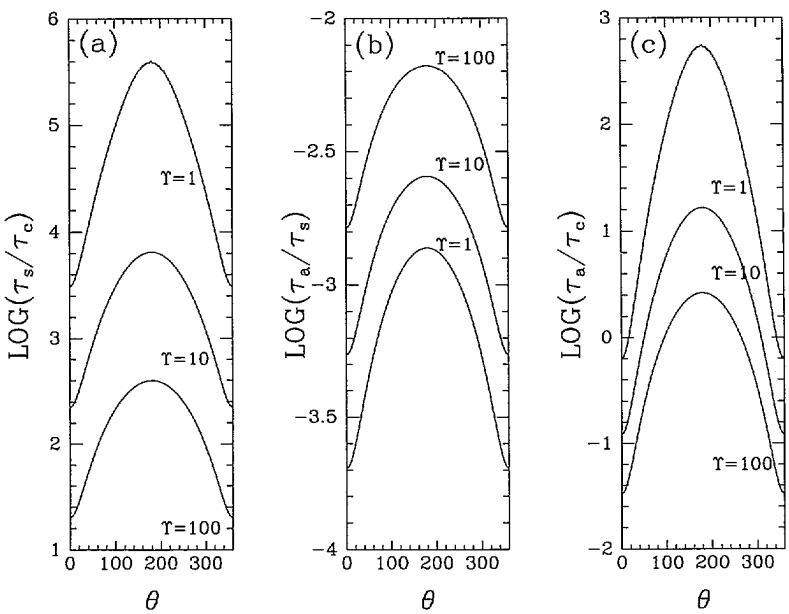

FIG. 2.—Logarithms of the ratios of (*a*) synchrotron loss time τ_s to nonrelativistic inverse-Compton cooling time τ_c, (*b*) acceleration time τ_a to τ_s, and (*c*) acceleration time τ_a to τ_c as functions of the true anomaly θ for different values of the mass-loss parameter Υ.

synchrotron nebula at distances from the pulsar $r \gtrsim r_s$ is diffuse. As a result, the shocked wind radiates a nebular synchrotron spectrum with emissivity $j_\epsilon \propto \epsilon^{-1/2}$ (photon energy cm^{-3} s^{-1}). The nonthermal acceleration of pairs at the shock produces a power-law distribution of accelerated particles for the case of magnetosonic absorption of the ion's waves and the maximum Lorentz factor γ_m. Therefore, the energy spectrum is in the range $\epsilon_1 < \epsilon < \epsilon_m$, where $\epsilon_1 = 0.3\gamma_1^2\hbar\omega_c(B_2) \approx (0.05\ \mathrm{keV})(\eta/0.3)^2(Z/A)^2(n_8 v_6^2)^{1/2}(\sigma/0.005)^{1/2}$, with A being the average ion atomic number, ω_c being the $e^\pm$-pair cyclotron frequency corresponding to the critical energy of the single-particle synchrotron emissivity for pairs of energy $\gamma_1 m_\pm c^2$, and $\epsilon_m = \gamma_m^2\hbar\omega_c(B_2) \simeq (210\ \mathrm{MeV})(\eta/0.3)^2(n_8 v_6^2)^{1/2}(\sigma/0.005)^{1/2}$. Since most of the emission comes from the highest energy particles, the nonthermal part of the pair spectrum dominates the emission. For $N(\gamma) \propto \gamma^{-s}$, the bolometric luminosity of the flowing plasma is $L_w \approx V_s c n_\pm^{(nt)}\sigma_T(B_2^2/6\pi)\gamma_1^{s-1}\gamma_m^{3-s}(1-x^{3-s})/(1-x^{s-1})$, where σ_T is the Thomson cross section, $n_\pm^{(nt)}$ the number of pairs in the nonthermal part of the pair distribution function, $V_s = (kr_s)^3$ (with $k \geq 1$) is the volume occupied by the radiating wind downstream from the shock, and $x \equiv \gamma_1/\gamma_m = Zm_\pm/m_i$ (Arons & Tavani 1993). We estimate $n_\pm^{(nt)}$ by noting that the shock converts a fraction ε_a of the pulsar's energy loss into the energy of the nonthermal part of the pair spectrum. Therefore, it can be shown that in the downstream medium flowing with velocity V_f, $L_w \simeq 10^{34}(\sigma/0.005)(\varepsilon_a/0.2)(\eta/0.3)(n_8 v_6^2/f_p^3)^{1/2}(c/3/V_f)$ ergs s^{-1}. This emission might explain the X-ray flux detected near apastron (Cominsky et al. 1994).

4.2. *Nonthermal "Compact" Nebular Emission*

This is the case characterized by $\tau_s, \tau_c \ll \tau_f$ which applies to the pulsar passage near periastron. We distinguish two main radiative regimes.

1. *Case A.*—If $\tau_a \ll \tau_f, \tau_s, \tau_c$, then magnetosonic acceleration of $e^\pm$ pairs at the shock is possible, and the shock pair power-law distribution of energies is expected to extend from γ_1 to some γ_m^*. This case occurs only for a small r_s near the pulsar and for a large ram pressure from the Be star outflow, i.e., $\Upsilon \gtrsim 100$. From Figures 2*b* and 2*c* we obtain that synchrotron radiation may dominate the cooling near periastron with $\tau_a \ll \tau_s$ for $\Upsilon \gtrsim 10^3$, especially if $\gamma_1 \sim 10^6$ when the relativistic IC scattering timescale applies. In this case, the energy spectrum is peaked at $\epsilon_1 \simeq 0.3\gamma_1^2\hbar\omega_c(B_2) \simeq 10$ keV with emissivity $j_\epsilon \sim \epsilon^{-1}$ up to an energy $\epsilon_m \sim 40$ MeV.

2. *Case B.*—For values of $\Upsilon \lesssim 10^3$, IC scattering dominates the cooling, and the acceleration time τ_a becomes larger than τ_c (and $\tau_{c,r}$) as Figure 2*c* indicates. In this case, the energy distribution of downstream $e^\pm$ pairs resembles a relativistic Maxwellian with no power-law tail due to shock acceleration. The optical depth τ^* for nonrelativistic IC scattering can be estimated as $\tau_{nr}^* \sim \sigma_T U_p r_s/\bar{\epsilon} \sim 10 r_{s,12}$, where we used the estimate for the blackbody radiation energy density $U_p \sim (40\ \mathrm{ergs\ cm^{-3}})[(R_*/\bar{R}_s)/0.2]^2$. If IC scattering is predominantly in the Thomson regime, the photon spectrum has a Maxwellian shape, with most of the energy radiated near the peak energy $E_p \sim \gamma^2\bar{\epsilon}$. In the case of PSR B1259−63, the center-of-mass energy in the electron frame is $\bar{\epsilon}\gamma_1/(m_\pm c^2) \sim 4.5\gamma_{1,6}$, and the Thomson regime applies when $\gamma_1 \lesssim 10^5$. In this case, the peak energy can be $E_p \sim (45\ \mathrm{GeV})\gamma_{1,5}^2$. The total luminosity of the IC spectrum is $L_{C,nr} = (4/3)\sigma_T c U_p \tilde{f} N \tilde{k}\gamma_1^2$, where $\tilde{k}$ is a constant of order unity, $N \sim \dot{N}\bar{\tau}$ is the total number of $e^\pm$ pairs IC radiating per unit time, with $\dot{N} \sim \tilde{f}\dot{E}_R/\gamma_1 m_\pm c^2$ being the $e^\pm$-pair production rate, $\bar{\tau}$ being the residence time $\bar{\tau} \sim r_s/(c/3)$, and $\tilde{f}$ being the fraction of N $e^\pm$-pairs near the shock. The total number of $e^\pm$ pairs is $N \sim 10^{38} r_{s,12}\gamma_{1,6}^{-1}$, and from an estimate of the solid angle of particles streaming toward the Be star, $\tilde{f} \sim 0.1$. We obtain $L_{C,nr} \sim 5 \times 10^{35}(\tilde{f}/0.1)N_{38}\gamma_{1,5}r_{s,12}$ ergs s^{-1}. Alternately, if $\gamma_1 \sim 10^6$, as in the case of the Crab pulsar (Kennel & Coroniti 1984), the IC scattering is in the Klein-Nishina regime with maximum photon energy $E_{\max} \sim \gamma_1 m_\pm c^2 \simeq (500\ \mathrm{GeV})\gamma_{1,6}$. The IC luminosity is in this case, $L_{C,r} \sim (3/8)\sigma_T c U_p (m_\pm c^2/\bar{\epsilon})^2 \tilde{f} N[\ln(2\gamma_1\bar{\epsilon}/m_\pm c^2) + 1/2] \sim 6 \times 10^{34}[(R_*/\bar{R}_s)/0.2]^2(\tilde{f}/0.1)$ ergs s^{-1}. Note that the relativistic $e^\pm$ pairs of the pulsar wind can have their γ_1 lowered by IC scattering even before they reach the shock.

5. CONCLUSIONS

We have studied the characteristics of high-energy emission from the PSR B1259−63 system. As the pulsar approaches and leaves the periastron region, the characteristics of the pulsar cavity enshrouded in the Be star outflow and the resulting high-energy emission are predicted to vary. For intermediate values of Υ, the shock is relatively close to the pulsar, and the shock acceleration mechanism considered here predicts a power law in the X-ray and gamma-ray range observable by current high-energy missions. In particular, X-ray instruments (*ROSAT*, *ASCA* [*Astro D*]) with a threshold luminosity $L \sim 10^{33}$–10^{34} ergs s^{-1} should be able to detect even faint X-ray emission and monitor the time dependence of the luminosity and spectrum.

We have also showed that if the mass outflow parameter Υ is relatively small ($\Upsilon \lesssim 100$), IC scattering dominates the cooling, and the resulting high-energy spectrum is peaked in the range of MeV–GeV with small contributions from lower energy photons. The characteristics of the emission are in this case independent of the shock acceleration mechanism and depend only on the Lorentz factor of the relativistic particles in the pulsar wind. The estimated luminosity of the high-energy emission is in the detectable range of *CGRO* instruments, with threshold high-energy luminosity $L \sim 10^{34}$–10^{35} ergs s^{-1}.

For values of Υ even larger than 10^4, the ram pressure of the mass outflow can be large enough to overcome the radiation pressure of the pulsar, and accretion may occur if the centrifugal barrier is overcome. The resulting X-ray emission can be a direct probe of the local pressure and ultimately of the mass outflow rate at periastron. Monitoring of the X-ray and high-energy emission before and after periastron might sensibly constrain Υ and the pulsar wind parameters γ_1 and σ.

M. T. acknowledges support by the NASA grant GRO/PFP-91-23. J. A. was supported in part by NASA grant NAGW-2413 and NSF grant AST 91-15093.

REFERENCES

Arons, J. 1994, in preparation
Arons, J., & Tavani, M. 1993, ApJ, 403, 249
Blumenthal, G., & Gould, R. 1970, Rev. Mod. Phys., 42, 237
Cominsky, L., Roberts, M., & Johnston, S. 1994, ApJ, 427, 978
Gallant, Y., & Arons, J. 1994, ApJ, in press
Hoshino, M., Arons, J., Gallant, Y. A., & Langdon, A. B. 1992, ApJ, 390, 454
Johnston, S., Manchester, R. N., Lyne, A. G., Bailes, M., Kaspi, V. M., Qiao, G., & D'Amico, N. 1992, ApJ, 387, L37
Johnston, S., Manchester, R. N., Lyne, A. G., Nicastro, L., & Spyromilio, J. 1994, MNRAS, in press
Kennel, C. F., & Coroniti, F. V. 1984, ApJ, 283, 694
King, A. 1993, ApJ, 405, 727
Kochanek, C. 1993, ApJ, 406, 638
Waters, L. B. F. M. 1986, A&A, 162, 121
Waters, L. B. F. M., et al. 1988, A&A, 198, 200